Thin Solid Films xxx (xxxx) xxx–xxx

Contents lists available at ScienceDirect

Thin Solid Films

journal homepage: www.elsevier.com/locate/tsf

Solution-processed CuO thin films with various Cu^{2+} ion concentrations

Hoa Quang Nguyen[a], Dung Van Nguyen[b], Akihiko Fujiwara[c], Bui Nguyen Quoc Trinh[b,d,*]

[a] Vietnam National University, VNU University of Science, Faculty of Physics, 334 Nguyen Trai, Thanh Xuan, Hanoi, Viet Nam
[b] Vietnam National University, VNU Vietnam Japan University, Nanotechnology Program, Luu Huu Phuoc, Nam Tu Liem, Hanoi, Viet Nam
[c] Kwansei Gakuin University, School of Science and Technology, Department of Nanotechnology for Sustainable Energy, 2-1 Gakuen, Sanda, Hyogo 669-1337, Japan
[d] Vietnam National University, VNU University of Engineering and Technology, Faculty of Engineering Physics and Nanotechnology, 144 Xuan Thuy, Cau Giay, Hanoi, Viet Nam

ARTICLE INFO

Keywords:
Cupric oxide
p-type semiconductor
Solar cell
Solution deposition process figure of merit

ABSTRACT

Presented herein is a report on cupric oxide (CuO) thin films prepared on glass substrates by using a solution process with varying nominal concentrations of Cu^{2+} ions at 0.15 M, 0.20 M, and 0.25 M. X-ray diffraction patterns and scanning electron microscopy (SEM) micrographs were analyzed to evaluate the crystalline structure and surface morphology of the CuO thin films. The fabricated CuO thin films exhibited a single-phased monoclinic structure with (200) and (111) orientations. The grain size of the CuO thin films was observed to increase with higher concentration, by SEM observation. The electrical and optical properties of the CuO thin films were investigated using a four-probe measurement system and UV/VIS spectrometer, respectively. The thin films showed a minimum resistivity of 0.085 Ω cm corresponding to the 0.25 M concentration, and a bandgap energy ranging from 2.10 eV to 2.15 eV. In addition, the light-harvesting ability of CuO thin films was considered by the absorption figure of merit (*a-FOM*), in correlation with the global solar spectrum. A maximum *a-FOM* value of 12.79 Ω^{-1} cm^{-1} was attained for the sample with a Cu^{2+} ion concentration of 0.25 M.

1. Introduction

Hitherto, the cupric oxide (CuO) thin film has been extensively known as a typical p-type semiconductor with a bandgap energy near 2.1 eV. It has a monoclinic structure and is grouped with abundant non-toxic materials [1–5]. In general, CuO thin films are considered promising for applications in semiconductor and energy storage devices, and as a catalyst [6,7]. Owing to its bandgap value of around 2.0 eV, the CuO thin film is being employed to expand the spectrum of harvested light from ultraviolet to visible regions while exhibiting a superior photocatalytic efficiency [5,8]. The CuO thin film also enabled the design of a hole-transport (p-type) visible-light absorber layer in solar cells [1,5]. From this perspective, the light absorption ability of CuO thin films plays a key role in photocatalytic experiments and solar cell production. In addition, the absorption length [1] or absorption figure of merit (denoted as *a-FOM*) of CuO thin films should be considered when evaluating the film. However, there are only a few related articles [9,10].

Due to the aforementioned conceivable essentials, various techniques to fabricate CuO thin films, such as electro-deposition [11,12], thermal oxidation [13,14], solution processing [15–20], chemical vapor deposition [21], pulsed laser deposition [8,22], and reactive ion sputtering [23–25] have been developed. Among these methods, the solution-processed approach is simplest. It offers a rich advantage for fabrication because of its low-power and low-material consumption. Additionally, it allows deposition on flexible substrates under atmospheric pressure. However, for solution processing, the stabilizer for the formation of CuO precursors is limited to 2-methoxyethanol stirred vigorously at room temperature [15]. In our solution process, we utilized monoethanolamine (MEA) to stabilize and chelate with copper acetate via O-Cu-O bonds at 75 °C. This provides a unique alternative to the traditional process of depositing high-quality CuO thin films. It should be noted that the surface morphology of the CuO thin film, influences its optical and electrical properties, and depends strongly on the fabrication conditions [16–19]. In previous reports, the resistivity of CuO thin films prepared by a solution-processed method was relatively high. It varied from 10^1 to 10^2 Ω cm [16,17], and up to and 10^3 Ω cm [15,19]. Hence, a reduction in the resistivity is expected. The decrease in resistivity normally results from the increasing grain size and the decreasing of porosity of the thin films. Therefore, the reduction of carrier-scattering at the grain boundaries lessens the resistivity [16]. Hence, the deposition conditions must be investigated to minimize the resistivity of CuO thin films via increase in the grain size and/or decrease in porosity. This can be done by changing the film layers

* Corresponding author.
E-mail address: trinhbnq@vnu.edu.vn (B.N.Q. Trinh).

https://doi.org/10.1016/j.tsf.2018.03.036
Received 20 November 2017; Received in revised form 13 March 2018; Accepted 13 March 2018

[16,17], or raising the annealing temperature [20].

In this study, the precursor was diluted to the desired concentrations after the formation of a gel state. It was then spin-coated on glass substrates. Meanwhile, the annealing temperature was fixed at 550 °C due to the limitation of the glass substrate. The concentration of the chemical precursors, i.e., the ratio of the precursors to the solvent, was systematically changed to determine the optimum film quality for the absorption layer of photonic devices. The structural, morphological, optical, and electrical properties, as well as the absorption length and absorption figure of merit of the CuO thin films were examined for optimization.

2. Experimental Procedures

2.1. Precursor solution

To prepare the precursor solutions, copper (II) acetate salt and MEA were used as a raw material and stabilizer of the CuO films, respectively. Firstly, copper acetate salt and MEA were dissolved in pure ethanol (99%) followed by magnetic stirring at room temperature. The molecule ratio between the copper acetate salt and MEA was kept at 1:2 for optimum conditions. Furthermore, the nominal concentration of Cu^{+2} ions for varying precursor solutions was controlled at 0.15 M, 0.2 M, and 0.25 M. Thereafter, the precursor solution was heated at a temperature of 75 °C in a dry oven to form the molecular network. A dark-blue transparent solution was observed after an hour. Finally, the precursor solution was added to pure ethanol to regain its initial volume before being stored in a bottle. A bottle was consumed for every sample prepared to avoid undesirable contaminations. Based on initial findings, a solution with a Cu^{+2} ion concentration of 1.0 M produced a CuO thin film with a discontinuous surface. On the other hand, a concentration of 0.30 M or greater produced precipitates in the precursor solutions.

2.2. Preparation of CuO thin films

Commercial $20 \times 20\,mm^2$ glass substrates were cleaned with acetone and 0.5% HF solution to remove organic and metal dusts. Thereafter, the substrates were coated with the precursor solution prepared beforehand. The precursor solution was flattened on the surface of glass substrates, then spin-coated at a speed of 1500 rpm for 60 s. The samples were then dried in ambient atmosphere at 90 °C for 3 min for each layer. At the condensed gel state, the process was repeated optionally to deposit thin films with the expected thickness. After transforming from the gel state to the crystallization state, the samples were annealed at a temperature of 550 °C in atmospheric pressure for 30 min. The samples were labelled as 0.15 M Cu^{2+}, 0.20 M Cu^{2+}, and 0.25 M Cu^{2+}, corresponding to the nominal concentration of the Cu^{2+} ions in the precursor solutions. For the solution with 0.25 M concentration, the annealing temperature was varied as 350 °C, 450 °C, and 550 °C to determine the optimum condition for preparing high-quality CuO thin films.

2.3. Thin films characterization

The crystalline quality of the CuO thin films was analyzed using an X-ray diffractometer (Bruker D5005, Siemens) at room temperature, with Cu-Kα (λ = 1.54056 Å) radiation, parallel beam, and a scanning speed of 0.03°/s from 10 to 70°. The morphology of the CuO thin films was observed via scanning electron microscopy (Nova NANOSEM-450, FEI), with an operating voltage of 5 kV. The optical transmittance of the CuO thin films was determined using a UV/VIS spectrophotometer (UV 2450-PC, Shimadzu).

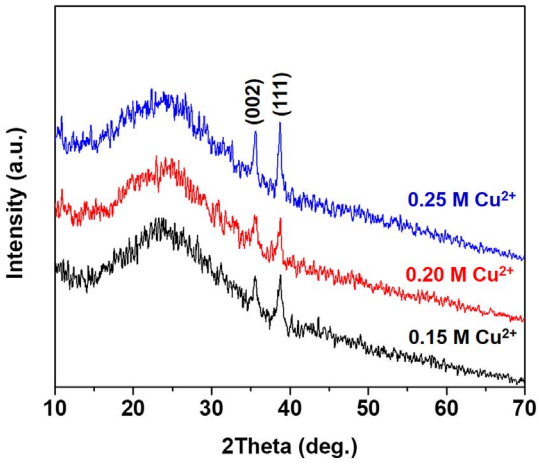

Fig. 1. XRD patterns of CuO thin films on glass substrates, with different Cu^{2+} ion concentrations.

3. Results and discussion

X-ray diffraction (XRD) patterns of the CuO thin film samples prepared with varying Cu^{2+} concentrations of precursors are shown in Fig. 1. Typical peaks appear at $2\theta = 35.6°$ and 38.7°, and are well-matched with the standard (002) and (111) orientations corresponding to the monoclinic crystal structure of CuO (JCPDS41-0254). No other significant phases were found in the XRD patterns, confirming that all samples mainly exhibit the CuO phase. Furthermore, the ratio of the peak intensities at 35.6° and 38.7° concurs with that of the peak intensities at (002) and (111) orientations based on standard patterns. This implies that the samples are polycrystalline, similar to another report on CuO thin films prepared using the sol-gel method [9]. Neglecting the peak broadening from equipment and/or from the residual stress of the thin films, the CuO crystallite size was derived using the Debye–Scherrer formula:

$$D = \frac{0.9\lambda}{\beta \cos\theta} \quad (1)$$

Here, λ and β are the X-ray wavelength and full width at half maximum of the peak at θ (Bragg angle), respectively. Consequently, the calculated crystallite sizes of the CuO thin films were 34 nm, 42 nm, and 46 nm, corresponding to the nominal concentrations of Cu^{2+} ions in the precursor solutions of 0.15 M, 0.20 M, and 0.25 M, respectively. The morphology of the CuO thin films was shown in Fig. 2. To determine the average particle size of CuO, we utilized a free software, ImageJ, to obtain the dependence of the percentage distribution on the particle size. Thereafter, using Gaussian fitting functions, the average particle size (D_{mean}) and standard deviation (ΔD) of the particle sizes were extracted (Figs. 2(d), (e) and (f)). D_{mean} was 28.4 ± 6.9 nm, 40.4 ± 5.4 nm, and 48.6 ± 5.9 nm for the 0.15 M, 0.20 M, and 0.25 M samples, respectively. Observably, the particle sizes derived by the ImageJ software and the Gaussian fitting functions, D_{mean}, agree well with those calculated by using the Debye–Scherrer formula. From these results, it can be inferred that the grain size of the particles on the thin film surface increases with the nominal Cu^{2+} ion concentration. Inset (i) in Fig. 2a shows the cross-sectional SEM image acquired to determine the thickness of the thin films. Empirically, the thickness of CuO thin films increases from 74 nm to 95 nm as the Cu^{2+} ion concentration increases from 0.15 M to 0.25 M, as summarized in Table 1. In addition, the CuO thin films become less porous as the film thickness increases, i.e., the surface of the thin films become denser. Therefore, if the Cu^{2+} ion concentration is chosen as 0.25 M, a CuO thin film with a non-porous surface can be achieved. This will be discussed subsequently. During the first step of gel formation, the Cu^{2+} ions react with MEA and form a 4-species complex [26] linking copper ions together.

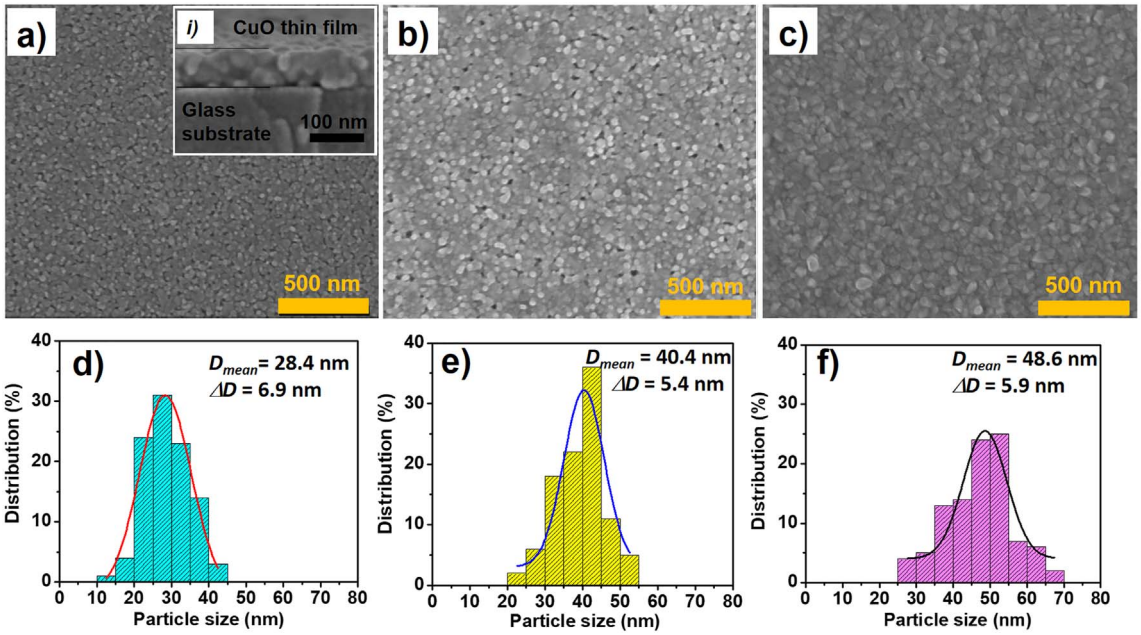

Fig. 2. SEM micrographs of CuO thin films for various Cu^{2+} ion concentrations: (a) 0.15 M, (b) 0.20 M and (c) 0.25 M. Dependence of percentage distribution on particle size calculated by using ImageJ software and fitted by Gaussian functions: (d) 0.15 M, (e) 0.20 M and (f) 0.25 M. Inset of (a) shows a cross section for the case of 0.15 M sample.

Table 1
Essential parameters of CuO thin films obtained for various Cu^{2+} ion concentrations.

Samples	0.15 M	0.20 M	0.25 M
Thickness (nm)	74	82	95
Resistivity (Ω cm)	1.707	0.137	0.085
Band gap (eV)	2.15	2.12	2.10
Absorption figure of merit (Ω^{-1} cm^{-1})	1.02	11.39	12.79

For the same volume, a lower concentration of the Cu^{2+} ion produces a lower concentration of the complex. After post-heating at 90 °C and annealing at 550 °C, CuO particles with smaller sizes are formed. Consequently, these cannot fill the spaces in the thin films. On the other hand, at a higher nominal concentration of Cu^{2+} ions, the CuO particles are larger and denser. At 0.25 M, the concentration of the complexes completely fills up the voids within the thin films. Hence, dense thin films with low porosity are well formed.

Because the transmittance of thin films is sensitive to the film thickness, only the highest average transmittance in the visible wavelength region was considered for the sample with 0.25 M. The absorption coefficient of the thin films was calculated using the Beer–Lambert Formula (1), i.e.,

$$\alpha = -\frac{\ln T}{d} \tag{2}$$

where, T and d are the transmittance and thickness of the thin film, respectively. This computation is plotted in Fig. 3a. At the region of interest, it can be visualized that the absorption coefficient of the thin films prepared from 0.25 M Cu^{2+} ion concentration is higher than those of the thin films from a concentration of either 0.15 M or 0.20 M. The results can be qualitatively explained using the relation,

$$\alpha = -\frac{\ln T}{\varepsilon} \tag{3}$$

where ε is the characteristic extinction coefficient of the thin-film material, and C is the concentration of the precursor solution indicative of how dense the thin film would be. The higher absorption coefficient of the 0.25 M sample signifies that it has higher opacity than the samples prepared from lower Cu^{2+} ion concentration. This is further supported by the SEM micrographs in Fig. 2.

The optical bandgap energy can be determined by using an extrapolation function, for which the Tauc relationship was used as follows [16]:

$$\alpha h\nu = A(h\nu - E_g)^2 \tag{4}$$

Here, α is the absorption coefficient, h is Planck's constant, ν is the photon frequency, and E_g is the optical-direct bandgap energy. An extrapolation of the linear region to the x axis, plotted in the graph of $(\alpha h\nu)^2$ versus photon energy, $h\nu$, gives the value of E_g, as shown in Fig. 3b. From this figure, E_g can be extracted to be 2.15 eV for the 0.15 M sample. However, this is reduced to 2.10 eV for the 0.25 M sample (details shown in Table 1). Although CuO is well-known as an electrical p-type semiconductor with indirect bandgap [27–29], a previous study reveals that the optical direct bandgap can be calculated. This suggests a directly allowed inter-band transition of the material [1]. The E_g of CuO has been reported to be approximately 2.1 eV [2,4], which shows that our findings are comparable with others. In addition, in our case, the decrease of the bandgap indicates the improvement of the thin films in electrical properties. Furthermore, the shifts of E_g might be due to the decrease of the defects in the thin films.

A four-probe measurement system at room temperature was used to investigate the variation of the electrical resistivity for the CuO thin films, with the results shown in Table 1. The sheet resistance was 230 kΩ/sq. This value was normalized to a resistivity of 1.707 Ω cm for the 0.15 M sample. However, the sheet resistance decreased to 17 kΩ/sq (or a resistivity of 0.137 Ω cm) for the 0.20 M sample. It further diminished to a resistance of 9 kΩ/sq (or a resistivity of 0.085 Ω cm) for the 0.25 M sample. Hence, the resistivity decreased with the increase of Cu^{2+} ion concentration; this is attributed to the improvement of the optical bandgap. Furthermore, when the grain size increases, the grain boundary decreases. Subsequently, the scattering of the carriers at the grain boundaries is limited. Ultimately, this improves the conductivity of the thin films, i.e., decreases the value of the resistivity. A resistivity of 0.085 Ω cm is one or two orders lower than values reported in other studies that employed solution processes [15,16]. In order to interpret this result, we consider the Cu^{2+} defects and/or the addition of O^{2-} interstitial sites. Based on the Drude model, $\sigma = (ne^2\tau)/m = (ne^2l)/(mv)$, where n, e, τ, m, v and l are the number of carriers, element charge, mean-free time, effective mass, group velocity, and mean-free

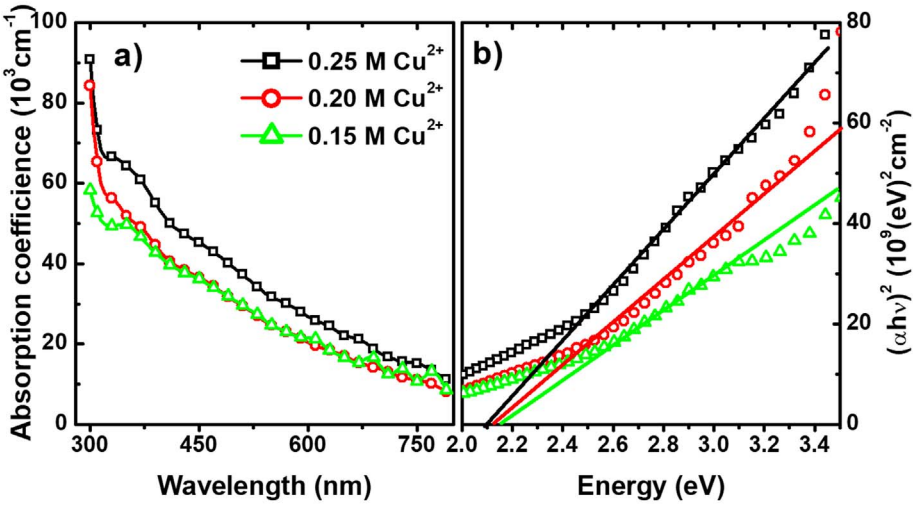

Fig. 3. Variation of absorbance spectra (a) and Tauc graphs (b) plotted as a function of Cu^{2+} ion concentrations.

path, respectively. It is assumed that *m* and *v* would not be significantly affected by the variation of the solution concentration. Therefore, it is plausible that the existence of charges between grains is much higher than that within the grains. Thus, an increase in the mean free path considerably enhances the conductivity of the thin films. Although the number of carriers also contributes to the conductivity, the sharp drop in the resistance of the films should not be attributed to a minute change in the number of carriers. The number of carriers, as well as the origin of the Cu^{2+} defects and/or excess O^{2-} at the interstitial sites, will be investigated in the next step using high quality films that were hardly affected by the grain boundary effect.

Fig. 4 shows the absorption rate (in percentage) of the thin films under ultraviolet (UV)-visible light. The average absorption rate of CuO thin films is relatively high at 55–80% at high photon energy, but is only 10–20% in the near-infrared (NIR) region. In this work, we considered the global spectrum of sunlight at 37 °C. The data were obtained from the American Society for Testing and Materials for photovoltaic performance evaluation. The sun illuminates less flux in the UV region and maximum flux at the visible region, but decreases as the photon energy decreases. Ideally, the optimal absorption for harvesting of natural light should have the same spectra with the solar flux. Fig. 4 shows how the CuO thin films displayed a fine absorption ability in the visible and NIR region, but a highly unwanted absorption in the UV region. Therefore, in order to evaluate the light harvesting ability of the conductive oxide thin films, the absorption length L_a is considered using the following Formula (1):

$$\frac{1}{L_\alpha} = \frac{\int_{Eg}^{\infty} \alpha(E) u_{ph}(E) dE}{\int_{Eg}^{\infty} u_{ph}(E) dE} \quad (5)$$

L_a is a characteristic factor indicative of which material can harvest solar light effectively. *α(E)* is the absorption coefficient as a function of the photon energy, and $u_{ph}(E)$ is the photon flux. Apart from L_a, the figure of merit was also determined by [9,10]:

$$F = (-\rho \ln T)^{-1} = (\rho \alpha d)^{-1} \quad (6)$$

where, ρ is the electrical resistivity. However, in Eq. (6), the figure of merit computation excludes the solar flux spectrum, implying that it is not related to the nature of light harvesting ability. Therefore, we introduce an absorption figure of merit (so-called *a-FOM*) for non-solar cells, which includes the solar flux spectrum. By combining Eqs. (5) and (6), the following equation can be obtained:

$$a - FOM = \langle \rho \alpha d \rangle^{-1} = \left(\frac{\int_{Eg}^{\infty} \rho d\alpha(E) u_{ph}(E) dE}{\int_{Eg}^{\infty} u_{ph}(E) dE} \right) = \left(\rho d \frac{1}{L_\alpha} \right) = \frac{L_\alpha}{\rho d} \quad (7)$$

The *a-FOM* must be favorable for the absorption layer in dark surfaces, like CuO thin films in photonic devices. Fig. 5 shows the dependence of both L_a (calculated from Eq. (5) and *a-FOM* (based on Eq. (7)) on the Cu^{2+} ion concentration. The black circles represent the L_a values, while the blue squares are for *a-FOM*. The L_a value was 122 nm for the 0.15 M sample, 121 nm for the 0.20 M sample, and 99 nm for the 0.25 M sample. On the other hand, *a-FOM* showed a positive correlation with a value of 1.02 Ω^{-1} cm^{-1} for the 0.15 M sample, 11.39 Ω^{-1} cm^{-1} for the 0.20 M sample, and 12.79 Ω^{-1} cm^{-1} for the 0.25 M sample (see Table 1). Additionally, using an optimum concentration of 0.25 M, the values of *a-FOM* and L_a were evaluated at various annealing temperatures of 350 °C, 450 °C, and 550 °C, as shown in the inset of Fig. 5. However, detailed data regarding the crystallization, surface morphology, and optical and electrical properties will be presented elsewhere. The *a-FOM* of the sample (i.e., the 0.25 M sample) at 550 °C is higher than that obtained at 350 °C and 450 °C. According to these

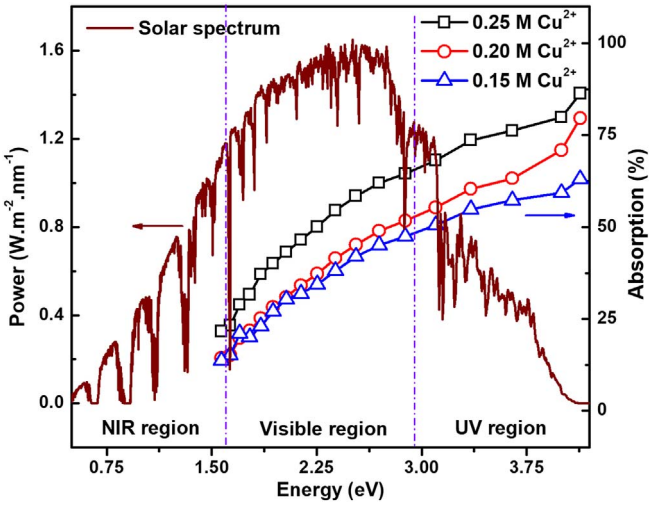

Fig. 4. Absorption spectra of CuO thin films corresponded to different Cu^{2+} ion concentrations measured from 300 nm to 800 nm (point-line experimental data) and global solar spectrum (brown curve), referred from the G137 standard spectrum of American Society for Testing and Materials for the evaluation of photovoltaic performance. (For interpretation of the references to colour in this figure legend, the reader is referred to the web version of this article.)

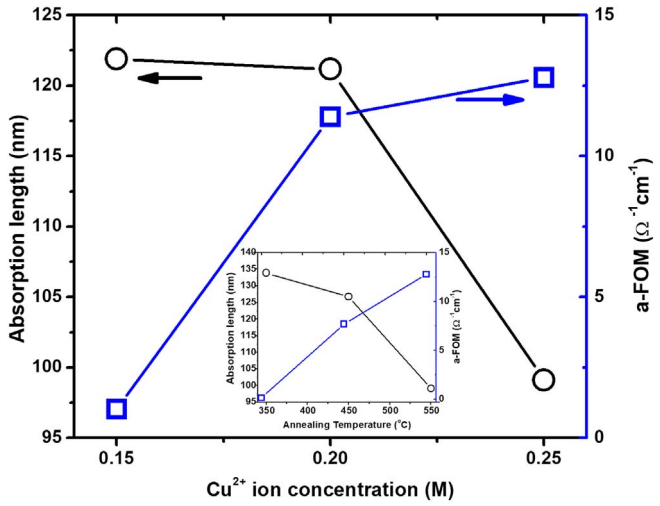

Fig. 5. Absorption length (circle) and absorption figure of merit (square) of CuO thin films depend on Cu^{2+} ion concentration. The inset is dependence of absorption length and absorption figure of merit on annealing temperature for the concentration of 0.25 M.

results, a temperature of 550 °C and concentration of 0.25 M is preferred for the deposition of high-quality CuO thin films. Accounting for the small difference in bandgap energy and a clear improvement in conductivity, the increment of *a-FOM* with Cu^{2+} ion concentration and annealing temperature is mainly attributed to the lower resistivity of denser thin films. Thus, the experimental results reveal that a Cu^{2+} ion concentration of 0.25 M and an annealing temperature of 550 °C are optimum for the fabrication of high-quality CuO thin films. The large value of *a-FOM* reflects a p-type semiconductor layer best used for harvesting natural light.

4. Conclusion

Solution-processed CuO thin films were prepared and investigated with various Cu^{2+} ion nominal concentrations. XRD results confirmed that the CuO thin films were single-phased with monoclinic structure and oriented along the (200) and (111) directions. The SEM micrographs showed that the average grain size in the CuO thin films ranges from 28.4–48.6 nm. Moreover, the thickness of the CuO thin films increased with Cu^{2+} ion concentration. Based on the absorbance spectra, the bandgap energies of the CuO thin films were 2.10 eV for 0.25 M, 2.12 eV for 0.20 M, and 2.15 eV for 0.15 M. The minimum electrical resistivity of the CuO thin films was 0.085 Ω cm for the 0.25 M sample. The absorption length (L_a) and absorption figure of merit (*a-FOM*) were 99 nm and 12.79 $\Omega^{-1}\,cm^{-1}$, respectively. The results suggest a promising technique to produce p-type absorption layers for solar cell applications.

Acknowledgments

The authors would like to thank Mr. Luu Manh Quynh for his valuable discussion on data analysis. This research is funded by Vietnam National Foundation for Science and Technology Development (NAFOSTED) under grant number 103.02-2012.81.

References

[1] F. Alharbi, J.D. Bass, A. Salhi, A. Alyamani, H.C. Kim, R.D. Miller, Abundant non-toxic materials for thin film solar cells: alternative to conventional materials, Renew. Energy 36 (2011) 2753–2758.
[2] T. Dimopoulos, A. Peic, P. Mullner, M. Neuschitzer, R. Resel, S. Abermann, M. Postl, E.J.W. List, S. Yakunin, W. Heiss, H. Bruckl, Photovoltaic properties of thin film heterojunctions with cupric oxide absorber, J. Renewable Sustainable Energy 5 (2013) 011205.
[3] B. Singh, S.K. Tiwary, CuO thin film prepared by chemical bath deposition technique: a review, J. Nanosci. Nanotechnol. 8 (2017) 11–15.
[4] K.S. Wanjala, W.K. Njoroge, N.E. Makori, J.M. Ngaruiya, Optical and electrical characterization of CuO thin films as absorber material for solar cell applications, Condens. Matter Phys. 6 (2016) 1–6.
[5] K.S. Khashan, A.I. Hassan, A.J. Addie, Characterization of CuO thin films deposition on porous silicon by spray pyrolysis, Surf. Rev. Lett. 23 (2016) 1650044.
[6] S.M. Panah, M. Kakran, Y.F. Lim, C.S. Chua, H.R. Tan, G.K. Dalapati, Graphene nanoparticle incorporated CuO thin film for solar cell application, J. Renewable Sustainable Energy 8 (2016) 043507.
[7] X.P. Gao, J.L. Bao, G.L. Pan, H.Y. Zhu, P.X. Huang, F. Wu, D.Y. Song, Preparation and electrochemical performance of polycrystalline and single crystalline CuO nanorods as anode materials for Li ion battery, J. Phys. Chem. B 108 (2004) 5547–5551.
[8] K. Osako, K. Matsuzaki, H. Hosono, G. Yin, D. Atarashi, E. Sakai, T. Susaki, M. Miyauchi, Examination of interfacial charge transfer in photocatalysis using patterned CuO thin film deposited on TiO_2, APL Mater. 3 (2015) 104409.
[9] J.J. Loferski, Thin films and solar energy applications, Surf. Sci. 86 (1979) 424–443.
[10] S. Cho, Optical and electrical properties of CuO thin films deposited at several growth temperatures by reactive RF magnetron sputtering, Met. Mater. Int. 19 (2013) 1327–1331.
[11] P. Poizot, C.J. Hung, M.P. Nikiforov, E.W. Bohannan, J.A. Switzer, An electrochemical method for CuO thin film deposition from aqueous solution, Electrochem. Solid-State Lett. 6 (2003) C21–C25.
[12] N. Mukherjee, B. Show, S.K. Maji, U. Madhu, S.K. Bhar, B.C. Mitra, G.G. Khan, A. Mondal, CuO nano-whiskers: electrodeposition, Raman analysis, photoluminescence study and photocatalytic activity, Mater. Lett. 65 (2011) 3248–3250.
[13] X. Jiang, T. Herricks, Y. Xia, CuO nanowires can be synthesized by heating copper substrates in air, Nano Lett. 2 (2002) 1333–1338.
[14] D. Tahir, S. Tougaard, Electronic and optical properties of Cu, CuO and Cu_2O studied by electron spectroscopy, J. Phys. Condens. Matter 24 (2012) 175002.
[15] Y.F. Lim, C.S. Chua, C.J.J. Lee, D. Chi, Sol–gel deposited Cu_2O and CuO thin films for photocatalytic water splitting, Phys. Chem. Chem. Phys. 16 (2014) 25928–25934.
[16] S.S. Shariffudin, S.S. Khalid, N.M. Sahat, M.S.P. Sarah, H. Hashim, Preparation and characterization of nanostructured CuO thin films using sol-gel dip coating, Mater. Sci. Eng. 99 (2015) 012007.
[17] H. Hashim, S.S. Shariffudin, P.S.M. Saad, H.A.M. Ridah, Electrical and optical properties of copper oxide thin films by sol-gel technique, Mater. Sci. Eng. 99 (2015) 012032.
[18] A. Bera, K. Deb, K.K. Chattopadhyay, R. Thapa, B. Saha, Mixed phase delafossite structured p type $CuFeO_2$/CuO thin film on FTO coated glass and its Schottky diode characteristics, Microelectron. Eng. 162 (2016) 23–26.
[19] N. Serin, T. Serin, S. Horzum, Y. Celik, Annealing effects on the properties of copper oxide thin films prepared by chemical deposition, Semicond. Sci. Technol. 20 (2005) 398–401.
[20] M.R. Das, A. Mukherjee, P. Mitra, Effect of annealing on structural, optical and electrical properties of SILAR synthesized CuO thin film, AIP Conf. Proc. 1832 (2017) 080016.
[21] T. Maruyama, Copper oxide thin films prepared by chemical vapor deposition from copper dipivaloylmethanate, Sol. Energy Mater. Sol. Cells 56 (1998) 85–92.
[22] A. Chen, H. Long, X. Li, Y. Li, G. Yang, P. Lu, Controlled growth and characteristics of single-phase Cu_2O and CuO films by pulsed laser deposition, Vacuum 83 (2009) 927–930.
[23] A.S. Reddy, H.-H. Park, V.S. Reddy, K.V.S. Reddy, N.S. Sarma, S. Kaleemulla, S. Uthanna, P.S. Reddy, Effect of sputtering power on the physical properties of dc magnetron sputtered copper oxide thin films, Mater. Chem. Phys. 110 (2008) 397–401.
[24] F. Klein, R. Pinedo, P. Hering, A. Polity, J. Janek, P. Adelhelm, Reaction mechanism and surface film formation of conversion materials for Lithium- and Sodium-ion batteries: an XPS case study on sputtered copper oxide (CuO) thin film model electrodes, J. Phys. Chem. C 120 (2016) 1400–1414.
[25] S. Dolai, R. Dey, S. Das, S. Hussain, R. Bhar, A.K. Pal, Cupric oxide (CuO) thin films prepared by reactive d.c. magnetron sputtering technique for photovoltaic application, J. Alloys Compd. 724 (2017) 456–464.
[26] E. Casassas, L.L. Gustems, R. Tauler, Spectrophotometric study of complex formation in copper(II) mono-, di-, and tri-ethanolamine systems, J. Chem. Soc. Dalton Trans. (1989) 569–573.
[27] A. Filippetti, V. Fiorentini, Magnetic ordering in CuO from first principles: a cuprate antiferromagnet with fully three-dimensional exchange interactions, Phys. Rev. Lett. 95 (2005) 086405.
[28] M. Nolan, S.D. Elliott, The p-type conduction mechanism in Cu_2O: a first principles study, Phys. Chem. Chem. Phys. 8 (2006) 5350–5358.
[29] F.P. Koffyberg, F.A. Benko, A photoelectrochemical determination of the position of the conduction and valence band edges of p-type CuO, J. Appl. Phys. 53 (1982) 1173.